Method to calculate the moments of the membrane voltage in a model neuron driven by multiplicative filtered shot noise

Lars Wolff and Benjamin Lindner
Max-Planck-Institut für Physik Komplexer Systeme, Nöthnitzer Strasse 38 01187 Dresden, Germany
(Received 8 August 2007; revised manuscript received 10 February 2008; published 17 April 2008)

Neurons are subject to synaptic inputs from many other cells. These inputs consist of spikes changing the conductivity of the target cell, i.e., they enter the neural dynamics as multiplicative shot noise. Up to now, only for simplified models like current-based (additive-noise) point neurons or models with Gaussian white-noise input, exact solutions are available. We present a method to calculate the exact time-dependent moments for the voltage of a point neuron with conductance-based shot noise and a passive membrane. The exact solutions show features (for instance, maxima of the moments vs time) which are also confirmed by numerical simulations. The theoretical analysis of subthreshold membrane fluctuations may contribute to a better comprehension of neural noise in general. We also discuss how the analytical results may provide additional conditions for estimating parameters from experimental data.

DOI: 10.1103/PhysRevE.77.041913 PACS number(s): 87.19.L−, 05.40.−a

I. INTRODUCTION

Neurons receive action potentials from many other cells. The timing of these *input spikes* appears in many cases to be rather irregular and can thus be described by a stochastic point process. This stream of input spikes called shot noise does not only lead to irregular spiking of the target neuron but also results in stochastic fluctuations of the subthreshold membrane voltage (i.e., below the threshold for generation of action potentials). From the statistics of these subthreshold fluctuations, one can obtain valuable information about the network and the synaptic dynamics (see, for instance, [1]), if a good theoretical description of the underlying dynamics is available. Moreover, a theoretical examination of the stochastic subthreshold behavior of neurons can help one to understand aspects of information processing in neurons.

For the last 50 years, many models for the subthreshold behavior of neurons have been studied. They cover a wide range from biophysically realistic multicompartment models (see, e.g., [2]), which incorporate many types of synapses and their distribution over the dendrite to very simple point neurons with voltage-independent additive Gaussian white noise (see, e.g., [3]). The model considered here lies somewhere in between. It is a shot-noise-driven passive (i.e., nonspiking) point neuron, which is described by the current-balance equation for a leaky capacitor and some fluctuating conductances [4]. The conductances are modeled by a linear filter equation with additive shot noise (throughout this paper, we mean by shot noise, the train of input delta spikes). Thus, one has to deal with a set of coupled differential equations driven by a multiplicative colored noise with non-Gaussian statistics. Even though this model is quite intuitive, the evaluation of the resulting equations is nontrivial. Up to now several groups have worked on approximations of this process, e.g., the diffusion approximation (see, e.g., [3,5–8]) and the effective time-constant approximation (ECA) [9,10]. A perturbation result (valid for small shot-noise amplitude) beyond the diffusion approximation and the ECA for steady-state densities and moments was recently presented by Richardson and Gerstner [11] (this paper also gives a comprehensive review on both diffusion approximation and ECA). So far, no exact results for this dynamics have been obtained.

The subthreshold activity can be measured experimentally *in vivo* and *in vitro* (see, e.g., [12,13]) in a standard procedure. One crude way to obtain the subthreshold fluctuations from measured trajectories is to cut the spikes generated by the neuron out of the voltage trace. Closer to what we are studying here are experiments in which the cell is hyperpolarized by a negative current and synaptic input is weak; the membrane is largely passive and does not generate action potentials.

In this paper, we propose a method which allows for the exact calculation of arbitrary n-time moments for the full problem, if the characteristic or the generating functional of the input noise is known. We show that the time-dependent moments (including also the voltage's autocorrelation function) can be expressed by the generating functional of the shot noise. The test function appearing in this functional depends on the synaptic filter dynamics. The resulting expressions for the moments can be evaluated in a lengthy but straightforward calculation.

As an application of this method, we calculate the mean value of the fluctuations for excitatory Poissonian input noise filtered by the synaptic dynamics. The variance and correlation function is discussed elsewhere.

This paper is organized as follows. In Sec. I A, we introduce the model. Some statistical quantities of interest are introduced in Sec. I B. In Sec. I C, we discuss some approximations of this model and their drawbacks. In the next two sections (Secs. II A and II B), we derive the formulas for the exact moments and we give a simple example in Sec. III. For this example, the limit of vanishing synaptic time scale is discussed in Sec. III B and conditions for a nonmonotonic time course of the mean are derived in Sec. III C. Finally, in Sec. III D, we compare the exact solutions to results of numerical simulations of the full problem. Our results are summarized and discussed in Sec. IV.

A. Model

We consider a shot-noise-driven passive point neuron as proposed by Stein [4]. The excitatory and inhibitory conduc-

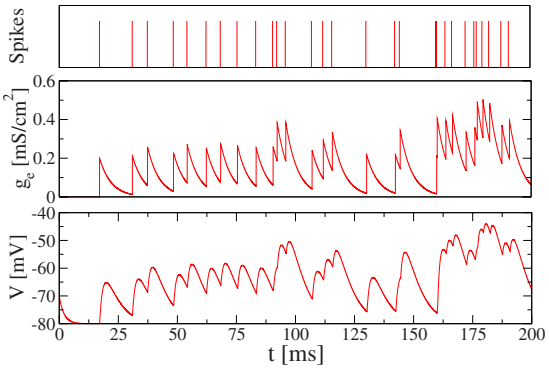

FIG. 1. (Color online) Example trajectories for the excitatory conductance and the membrane voltage. Here, only an excitatory Poissonian shot-noise input is present (no inhibition). The conductance g_e has jump discontinuities of fixed magnitude at the times of spike arrival t_k, whereas the voltage V changes smoothly with a magnitude proportional to the distance from the excitatory reversal potential $V-E_e$. The parameters used are $r_e=150$ Hz, $c_e=0.2$ mS/cm^2, $g_L=0.05$ mS/cm^2, $\tau_e=5$ ms, $C=0.1$ μF/cm^2, $E_e=0$ mV, and $E_L=-80$ mV.

tances are modeled by linearly filtered shot noise. This linear filter was used by Brunel and Sergi [14] for an additive dynamics and by Richardson and Gerstner [11] for a conductance (multiplicative) input, both for Poissonian shot noise. A similar model with unfiltered multiplicative Poissonian shot-noise input has been treated in [15]. In contrast to the previous works we do not make assumptions about the statistics of the shot noise except for its stationarity. The equations for the model considered here read

$$C\frac{dV}{dt} = -(V-E_L)g_L - (V-E_e)g_e(t) - (V-E_i)g_i(t) + I_{app}, \tag{1}$$

$$\tau_{e,i}\frac{dg_{e,i}}{dt} = -g_{e,i} + c_{e,i}\tau_{e,i}\sum_{\{t_{k_{e,i}}\}}\delta(t-t_{k_{e,i}}), \tag{2}$$

where C and g_L are the capacitance and the leakage conductance of the membrane, respectively, g_e and g_i are the excitatory and inhibitory fluctuating input conductances, respectively, and $\tau_{e,i}$ and $E_{e,i}$ are the respective time constants and reversal potentials, respectively. The parameters c_e and c_i determine the strength of the noise pulses, arriving at randomly distributed times $t_{k_{e,i}}$. We include an external current, represented by I_{app}. The fluctuating conductances should be considered as the sum over all respective ion channel conductances and are instantaneously changed by every spike, arriving at the respective (excitatory or inhibitory) synapse. The linear filter dynamics in Eq. (2) corresponds to a kinetic Markov scheme for the channel with two states ("open" and "closed") [16]; it has been found to be in good agreement with experimental data [17].

In Fig. 1, a visualization of Eqs. (1) and (2) is shown. The plot was generated from the simulation of an example trajectory with purely excitatory Poissonian shot-noise input. In the upper panel, the times of spike arrival, t_k, are indicated with vertical bars. The mid panel shows the respective time course of the excitatory conductance. Every time a spike arrives, the conductance makes a jump of fixed size and then relaxes toward zero until the next spike. In the lower panel, we show the voltage response to the conductance changes. With increasing conductance, the voltage goes smoothly toward the excitatory reversal potential (in this example 0 mV). Due to the multiplicative character, the amplitude of the voltage increase is not fixed, but decreases with the difference $V-E_e$. Thus, the one spike arriving at a time where the voltage is low, $t\approx 20$ ms, has a larger impact than the many spikes arriving at $t\approx 175$ ms, where the voltage is close to the excitatory reversal potential.

B. Time-dependent statistics of interest

The central quantity of interest in this paper is the nth time-dependent moment, defined by

$$\langle V(t_1)\cdots V(t_i)\cdots V(t_n)\rangle, \quad (t_n \geq t_{n-1} \geq \cdots \geq t_1 \geq 0). \tag{3}$$

Here the average is taken over an ensemble of equilibrated synaptic variables. This corresponds to the following initial conditions:

$$V(t=0) = V_0, \tag{4}$$

$$g_{e,i}(t\to-\infty) = y_0, \tag{5}$$

where y_0 is an arbitrary initial value that does not affect the dynamics for $t>0$ considered here. The rationale behind Eq. (5) is that while clamping the voltage at time $t=0$, we cannot control and will not influence the synaptic dynamics at the same time.

Experimentally or in a simulation, the first step in measuring the voltage moments would be to clamp the neuron's voltage to the value V_0. After releasing the voltage clamp, the trajectory is recorded. This has to be repeated many times to get an ensemble of time-dependent voltage traces. The moments of this ensemble are an estimate of the time-dependent moments of Eq. (1). The estimation procedure is illustrated in Fig. 2 for the time-dependent mean value in the case of just one excitatory synapse with Poissonian shot noise. Individual voltage traces (left panels) which all start at $V(t=0)=V_0$ are averaged, resulting in a curve that starts at V_0 and saturates in the long-time limit at the stationary mean voltage $\langle V\rangle_{st}$. The latter value as well as the exact time course between V_0 and $\langle V\rangle_{st}$ may reveal the multiplicative nature of the conductance noise, for instance, by a nonexponential or even a nonmonotonic run of the curve. We consider these cases below in more detail.

Our method also allows for the determination of membrane voltage statistics which *do not* require a repeated voltage clamp, i.e., which can be extracted from a long voltage recording only. The first obvious statistics of this kind would be the nth steady-state moment obtained by taking all times in Eq. (3) equal and letting t go to infinity. Furthermore, the stationary autocorrelation function can be expressed by the second and first time-dependent moments.

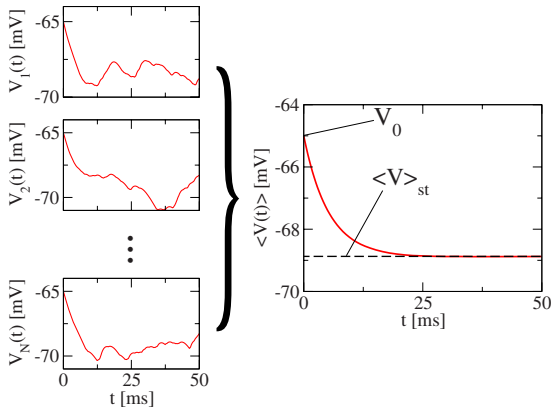

FIG. 2. (Color online) Estimate of the time-dependent moment $\langle V(t)\rangle$ (right panel) by averaging over an ensemble of trajectories (left panels) all started at $V(t=0)=V_0$. The asymptotic (stationary) mean voltage $\langle V\rangle_{st}$ is indicated. For this example we chose a purely excitatory input: a Poisson shot noise in the g_e dynamics with rate $r_e=1000$ Hz; other parameters: $E_e=-65$ mV, $E_L=-80$ mV, $\tau_e=3$ ms, $c_e=0.05$ mS/cm^2, $g_L=0.05$ mS/cm^2, $V_0=-65$ mV, and $C=1$ μF/cm^2.

C. Common approximations

For a Poissonian shot noise, one can, for high input rates ($r_{e,i}\tau_{e,i}\gg 1$), replace the point process in Eq. (2) with a continuous Gaussian process [3,11]. Under the same conditions, one can furthermore neglect the first-order multiplicative contributions of the input noise [9–11]. The resulting equations read [11]

$$C\frac{dV}{dt} = -(V-E_0)g_0 - (E_e-E_0)g_{eF}(t) - (E_i-E_0)g_{iF}(t), \tag{6}$$

$$\tau_{e,i}\frac{dg_{e,i;F}}{dt} = -g_{e,i;F} + \sqrt{2\tau_{e,i}}\sigma_{e,i}\xi_{e,i}(t), \tag{7}$$

where $g_0=g_L+g_{e0}+g_{i0}$, $E_0=1/g_0(E_L+E_e+E_i)$, and $\xi(t)$ is Gaussian white noise with $\langle\xi(t)\rangle=0$ and $\langle\xi(t)\xi(t')\rangle=\delta(t-t')$. Furthermore, the new parameters $g_{e,i0}=c_{e,i}\tau_{e,i}r_{e,i}$ and $\sigma_{e,i}=c_{e,i}\sqrt{\tau_{e,i}r_{e,i}/2}$ are introduced, which are equal to the mean and the variance of the original conductances, respectively.

The equations resemble a white-noise-driven current-based model with the membrane time scale replaced by an effective time scale $\tau_0=C/g_0$. Thus, this approximation is referred to as *effective time-constant approximation (ECA)* [9–11]. For this approximation, all moments can be computed easily. The time-dependent mean value predicted by the ECA is a simple exponential. With the initial condition $\langle V(0)\rangle=V_0$, it reads

$$\langle V(t)\rangle = (V_0-E_0)e^{(-g_0/C)t} + E_0. \tag{8}$$

Richardson and Gerstner stated that the ECA is valid for

$$\sigma_{e,i}/g_{e0,i0} = (2r_{e,i}\tau_{e,i})^{-1/2} \ll 1. \tag{9}$$

The ECA can be considered as a first-order expansion of the full dynamics in the small parameter equation (9). We note that the parameters c_e, c_i have to be small as well, i.e.,

$$c_{e,i} \ll g_L. \tag{10}$$

Compare also the paper of Burkitt and Clark [18], where an expansion for small excitatory postsynaptic potential amplitudes for additive synaptic noise has been introduced.

For later use, we would like to point out a remarkable feature of the ECA in our particular setup (equilibrated conductances): the ECA and the original process will yield the same short-time dynamics for the first moment as shown in Appendix A. Specifically, we show there that

$$\left.\frac{d\langle V\rangle}{dt}\right|_{t=0} = \left.\frac{d\langle V\rangle_{ECA}}{dt}\right|_{t=0}. \tag{11}$$

So looking at very short times after our initial clamping, the mean of the voltage is well described by the ECA. Deviations can be expected for moderate times and in the asymptotic limit, i.e., for the steady-state mean value. The latter has been calculated by Richardson and Gerstner [11] in a perturbation calculation that goes beyond the ECA. Their correction term reads

$$\langle V\rangle_\infty - E_0 = -\left(\sigma_e^2/g_0^2(E_e-E_0)\frac{\tau_e}{\tau_e+\tau_0} + \sigma_i^2/g_0^2(E_i-E_0)\frac{\tau_i}{\tau_i+\tau_0}\right). \tag{12}$$

In Sec. III, we compare the exact mean value for the full dynamics to the prediction of the ECA equation (8) and simulation results. Furthermore, the asymptotic values are compared to the results of the perturbation expansion [11] given above in Eq. (12).

II. GENERAL THEORY

If the input noise is white (e.g., a Poisson shot noise) we may write down an evolution equation for the voltage and the conductance which attains the form of a master equation with certain jump terms [3,19]. One can try to calculate the time-dependent moments from such an equation—either by explicit solution for the probability density itself (from which any moment can, in principle, be calculated) or by finding a (closed) set of equations for those moments.

Here we pursue a different approach which uses solely the original stochastic differential equations and does not assume that the input noise is white. Our idea is based on the following observation: the dynamics of the voltage as given in Eq. (1) is just a linear problem if we consider the conductance noise as a time-dependent parameter. Hence given a specific realization of the input noise, we can write down the well-known solution for a first-order linear differential equation with time-dependent coefficients. However, if we want to compute the statistics, we encounter averages of complicated functions of the input conductance noise. The main problem is to calculate these averages.

A. Equations for the exact *n*th order moments

In this section, we derive equations for moments of arbitrary order. To this end, we simplify Eqs. (1) and (2) by

shifting the variable V by E_L and renaming some parameters as follows:

$$v = V - E_L, \quad v_{e,i} = E_{e,i} - E_L, \quad v_0 = V_0 - E_L, \quad \beta = \frac{g_L}{C},$$

$$i_{app} = \frac{I_{app}}{C}, \quad y_{e,i}(t) = \frac{g_{e,i}(t)}{C}, \quad \varepsilon_{e,i} = \frac{c_{e,i}\tau_{e,i}}{C}. \tag{13}$$

While most of our new parameters were chosen for the ease of notation, the parameters $\varepsilon_{e,i}$ have a new meaning. They are nondimensional products of ratios

$$\varepsilon_{e,i} = \frac{c_{e,i}}{g_L}\frac{\tau_{e,i}}{C/g_L} = \frac{c_{e,i}}{g_L}\frac{\tau_{e,i}}{\tau_{mem}}, \tag{14}$$

where the first factor is the ratio of the increment of the conductance and the leak conductance of the unperturbed system and the second factor is the ratio of conductance filter time scale and membrane time constant (of the unperturbed system). This parameter is thus large for slow synapses and large jump amplitudes.

By means of the transformation in Eq. (13), we obtain the following new equations:

$$\frac{dv}{dt} = -\beta v - (v - v_e)y_e(t) - (v - v_i)y_i(t) - i_{app}, \tag{15}$$

$$\tau_{e,i}\frac{dy_{e,i}}{dt} = -y_{e,i} + \varepsilon_{e,i}\sum_{\{t_{k_{e,i}}\}}\delta(t - t_k). \tag{16}$$

Equation (15) is a linear first-order differential equation with time-dependent coefficients $y_e(t)$ and $y_i(t)$. Such an equation can be easily solved (see also [20]) and the formal solution reads

$$\begin{aligned} v(t) = v_0 \exp\left\{-\beta t - \int_0^t du[y_e(u) + y_i(u)]\right\} \\ + \int_0^t ds[v_e y_e(s) + v_i y_i(s) + i_{app}]e^{-\beta(t-s)} \\ \times \exp\left\{-\int_s^t du[y_e(u) + y_i(u)]\right\}. \end{aligned} \tag{17}$$

This can be written as

$$\begin{aligned} v(t) = v_0 e^{-\beta t - \int_0^t du[y_e(u)+y_i(u)]} + \int_0^t ds\Bigg[v_e e^{-\int_s^t y_i(u)}\frac{d}{ds}e^{-\int_s^t duy_e(u)} \\ + v_i e^{-\int_s^t duy_e(u)}\frac{d}{ds}e^{-\int_s^t duy_i(u)} + i_{app}e^{-\int_s^t du[y_e(u)+y_i(u)]}\Bigg]e^{-\beta(t-s)}. \end{aligned} \tag{18}$$

The nth time-dependent moment of this function reads

$$\begin{aligned} \langle v(t_1)v(t_2)\cdots v(t_n)\rangle = \Bigg\langle \prod_{m=1}^{n}\Bigg(v_0 e^{-\beta t_m - \int_0^{t_m} du[y_e(u)+y_i(u)]} \\ + \int_0^{t_m} ds\Bigg[v_e e^{-\int_s^{t_m} y_i(u)}\frac{d}{ds}e^{-\int_s^{t_m} duy_e(u)} \\ + v_i e^{-\int_s^{t_m} duy_e(u)}\frac{d}{ds}e^{-\int_s^{t_m} duy_i(u)} \\ + i_{app}e^{-\int_s^{t_m} du[y_e(u)+y_i(u)]}\Bigg]e^{-\beta(t_m - s)}\Bigg)\Bigg\rangle \end{aligned} \tag{19}$$

(knowing all moments up to order n, the nth moment of $V(t)$ can be obtained via $V(t)=v(t)+E_L$). After a lengthy calculation (see Appendix B), this expression reveals its key feature: All averages share one structure, namely,

$$\left\langle \exp\left[-\sum_j \int_{s_j}^{t_j} duy_{e,i}(u)\right]\right\rangle, \tag{20}$$

where the s_j are the respective integration variables if the factor stems from the inhomogeneous solution or zero if the factor stems from the homogeneous solution. In words, we have to average the exponential of a finite sum of integrals over the conductance noise—once this average is known, the moment can be computed in a straightforward way.

B. Evaluation of expression (20)

In the following, we show that expression (20) is strongly connected to the characteristic functional of the input noise. To this end, we have to rewrite the formal asymptotic solution of the linear filter equation for the incoming shot noise, Eq. (16), in terms of a Green's function as follows:

$$y_{e,i}(u) = \int_{-\infty}^{u} dt' \frac{\varepsilon_{e,i}}{\tau_{e,i}} e^{-(u-t')/\tau_{e,i}}\xi_{e,i}(t') \tag{21}$$

$$= \int_{-\infty}^{+\infty} dt' G_{e,i}(u - t')\xi_{e,i}(t'), \tag{22}$$

with $\xi_{e,i}(t) = \Sigma_{\{k_{e,i}\}}\delta(t - t_{k_{e,i}})$. $G_{e,i}$ is defined as

$$G_{e,i}(u - t') = H(u - t')\frac{\varepsilon_{e,i}}{\tau_{e,i}} e^{-u-t'/\tau_{e,i}}, \tag{23}$$

where $H(x)$ is the Heaviside function. The integral in Eq. (20) can now be written as

$$\sum_j \int_{s_j}^{t_j} duy_{e,i}(u) = \int_{-\infty}^{+\infty} dt'\left(\sum_j \int_{s_j}^{t_j} duG_{e,i}(u - t')\right)\xi_{e,i}(t') \tag{24}$$

(where we exchanged the order of integration) or

$$-\sum_j \int_{s_j}^{t_j} duy_{e,i}(u) = i\int_{-\infty}^{\infty} duU(u;\{t_j\},\{s_j\})\xi_{e,i}(u), \tag{25}$$

with

$$U(u;\{t_j\},\{s_j\}) = i\sum_j \int_{s_j}^{t_j} dt' G_{e,i}(t'-u). \tag{26}$$

Now we can insert Eq. (25) into Eq. (20) to obtain

$$\left\langle \exp\left[-\sum_j \int_{s_j}^{t_j} duy_{e,i}(u)\right]\right\rangle = \left\langle \exp\left[i\int_{-\infty}^{\infty} duU(u;\{t_j\},\{s_j\})\xi_{e,i}(u)\right]\right\rangle. \tag{27}$$

The structure of Eq. (27) is familiar. It is nothing else but the characteristic functional (see, e.g., the book of Stratonovich [21]) of the unfiltered input shot noise with a specific function defined by Eq. (26).

$$\left\langle \exp\left[-\sum_j \int_{s_j}^{t_j} duy_{e,i}(u)\right]\right\rangle = \Theta_{\xi_{e,i}}[U(u;\{t_j\},\{s_j\})]. \tag{28}$$

If we recapitulate the relation between the characteristic and the generating functional (see, e.g., [21]),

$$\Theta_{\xi_{e,i}}[U(t)] = L_{\xi_{e,i}}[e^{iU(t)}-1], \tag{29}$$

we also can connect Eq. (20) to the generating functional $L_{\xi_{e,i}}[U(u)]$. This means, to write down an expression for an arbitrary moment of the voltage fluctuations, it is sufficient to know the generating or the characteristic functional of the incoming unfiltered shot noise

$$\left\langle \exp\left[-\sum_j \int_{s_j}^{t_j} duy_{e,i}(u)\right]\right\rangle = \Theta_{\xi_{e,i}}\left[i\sum_j \int_{s_j}^{t_j} dt' G_{e,i}(t'-u)\right], \tag{30}$$

$$\left\langle \exp\left[-\sum_j \int_{s_j}^{t_j} duy_{e,i}(u)\right]\right\rangle = L_{\xi_{e,i}}\left\{\exp\left[-\sum_j \int_{s_j}^{t_j} dt' G_{e,i}(t'-u)\right]-1\right\}. \tag{31}$$

The filtering enters through the conductance's Green's function, Eq. (23). Methods to calculate the respective functionals can be found in [22].

III. APPLICATION: TIME-DEPENDENT MEAN FOR POISSONIAN INPUT

A. Analytical results

As an example, we calculate the exact mean value for only excitatory Poissonian shot-noise input; this means $y_i \equiv i_{app} \equiv 0$.

As explained above, we define the time-dependent mean as the ensemble average over many time-dependent voltage trajectories, each with initial value v_0. The fluctuating conductances, however, are assumed to be in a steady state, without memory of an initial value. The mean of Eq. (18) reads

$$\langle v(t)\rangle = v_0 e^{-\beta t}\langle e^{-\int_0^t duy_e(u)}\rangle + v_e \int_0^t ds e^{-\beta(t-s)} \frac{d}{ds}\langle e^{-\int_s^t duy_e(u)}\rangle. \tag{32}$$

The mean value appearing in this expression is a special case of expression (20). Because the generating functional for a homogeneous Poisson process is known [21],

$$L_{\xi_e;T_-,T_+}[U(t)] = e^{r_e\int_{T_-}^{T_+} dtU(t)}, \tag{33}$$

we can make use of Eq. (31). Expression (20) thus yields

$$\langle e^{-\int_s^t duy_e(u)}\rangle = \exp\left[r_e\int_{-\infty}^{+\infty} du(e^{-\int_s^t dt' G_e(t'-u)}-1)\right]. \tag{34}$$

In the following, the argument of the exponential in Eq. (34) is called f_e.

$$f_e(t,s) = r_e\int_{-\infty}^{+\infty} du(e^{-\int_s^t dt' G_e(t'-u)}-1). \tag{35}$$

As shown in detail in Appendix C, this expression depends only on the time difference $t-s$, i.e., $f_e(t,s)=f_e(t-s)$ where the explicit expression for f_e reads

$$f_e(t) = r_e\tau_e\{\mathcal{E}i[\varepsilon_e(e^{-t/\tau_e}-1)] + e^{-\varepsilon_e}\mathcal{E}i[\varepsilon_e] - \gamma - e^{-\varepsilon_e}\mathcal{E}i[\varepsilon_e e^{-t/\tau_e}] - \ln[\varepsilon_e(e^{t/\tau_e}-1)]\}. \tag{36}$$

Here $\mathcal{E}i[x]=-\int_{-x}^{\infty} dte^{-t}/t$ is the exponential integral function and γ denotes the Euler-Mascheroni constant, $\gamma = 0.577\,215\,66\ldots$. Putting everything together, we can write down the exact expression for the mean value

$$\langle v(t)\rangle = v_0\exp[-\beta t + f_e(t)] - v_e\int_0^t d\tau \exp[-\beta\tau + f_e(\tau)]\frac{df_e(\tau)}{d\tau}, \tag{37}$$

with f_e given by Eq. (36). We recall that the original dynamics can be obtained by using the transformations Eqs. (13).

For vanishing ε_e, the solution approaches the ECA solution Eq. (8) as can be seen as follows. For $\varepsilon_e \to 0$, the function $f_e(t)$ approaches [using expression (C9) given in Appendix C and keeping only the leading-order term]

$$f_e(t) \to -r_e\varepsilon_e t. \tag{38}$$

Inserting this into Eq. (37) yields Eq. (8) using all the abbreviations introduced in Sec. I C and transforming back to the original variables and parameters using Eqs. (13).

B. Special case: Unfiltered input noise ($\tau_e \to 0$)

To simplify the calculations, some authors have neglected the finite time constant of the conductances and consider an unfiltered shot noise, $g_e \propto \Sigma_{t_k}\delta(t-t_k)$ (see, for instance, [15,20]). This case is contained in our calculations as the limit of vanishing synaptic time constants τ_e while $\varepsilon_e = c_e\tau_e/C$ is kept constant. Only the f_e function, Eq. (36), is affected by this limit.

Due to the factor τ_e, in the brackets in Eq. (36) only terms of order $1/\tau_e$ have to be taken into account. The only terms

which do not become constant in this limit are the logarithm and $e^{-\varepsilon_e}\mathcal{E}i[\varepsilon_e e^{-t/\tau_e}]$, since the $\mathcal{E}i[x]$ function has a logarithmic divergence at $x=0$. For small arguments, the $\mathcal{E}i[x]$ function can be expanded according to $\mathcal{E}i[x]\approx\ln[|x|]+\gamma$. Performing this limit, Eq. (36) turns into

$$f_{e,i;\tau_e=0}(t) = r_e(e^{-\varepsilon_e}-1)t. \tag{39}$$

With Eq. (39), Eq. (37) yields

$$\langle v_{\tau_e=0}(t)\rangle = v_0 e^{-\omega t} - v_e \frac{r_e(1-e^{-\varepsilon_e})}{\omega}(e^{-\omega t}-1), \tag{40}$$

where $\omega=\beta+r_e(1-e^{-\varepsilon_e})$ is the new effective decay time constant. The solution is very similar to the ECA solution Eq. (8)—indeed the latter is obtained if the exponential is expanded in ε_e to first order.

For vanishing ε_e, $\omega=\beta$, whereas for large ε_e, it approaches $\beta+r_e$. The asymptotic value of Eq. (40) depends strongly on the input rate r_e. For very low rates, the asymptotic value equals the leakage reversal potential. On the other hand, for very high rates, the asymptotic value approaches the synaptic reversal potential.

Our result Eq. (40) is similar to that by Tuckwell [15] [cf. Eq. (14) therein] who obtained the time-dependent mean of the voltage using a probability-density approach. Tuckwell, however, used another interpretation of the stochastic differential equation (the analog of an Ito interpretation for a stochastic differential equation with white Gaussian noise). Our approach corresponds to the Stratonovich interpretation which assumes that the input noise is not really a true white noise but only the limit of a colored noise with negligibly small correlation time (see Gardiner [23], Sec. 6.5). The differences between the two interpretations are very small as long as the amplitudes $\varepsilon_{e,i}$ are small (see Ref. [20]).

C. Conditions for a nonmonotonic mean

To investigate possible shortcomings of the ECA, it is convenient to look for a nonmonotonic behavior for the exact mean value (the ECA predicts a purely monotonic time course; see Sec. I C). This we may find from our analytical result by setting $d\langle v(t)\rangle/dt|_{t=t_m}=0$, where t_m is the instant of the extremum. This leads to the equation

$$1-e^{-A} = A/b, \tag{41}$$

with $A=\varepsilon_e(1-e^{-t_m/\tau_e})$ (which is always positive for $t_m>0$) and $b=r_e\varepsilon_e(v_e-v_0)/v_0\beta$. From the latter equation, we can find conditions for the appearance of maxima in the time course: By graphical interpretation of the equation, it becomes clear that the functions on the left-hand side and the right-hand side of Eq. (41) can only intersect if the slope $1/b$ of the linear function is smaller than 1, i.e., $b>1$.

Furthermore, it can be shown that $(1-e^{-A})/A$ is a monotonically decreasing function of A. Since $A<\varepsilon_e$ we obtain from Eq. (41),

$$\frac{1}{b} = \frac{1-e^{-A}}{A} > \frac{1-e^{-\varepsilon_e}}{\varepsilon_e}. \tag{42}$$

Both conditions can be expressed in terms of v_0. For the necessary algebraic manipulations, we had to use (i) $v_0>0$, i.e., $V_0>E_L$ and (ii) $v_0<v_e$, i.e., $V_0<E_e$ (both follow, for excitatory input, from $b>0$ which is implied in the condition $b>1$ derived above). The conditions are summarized in the following useful inequality:

$$\frac{r_e(1-e^{-\varepsilon_e})v_e}{\beta+r_e(1-e^{-\varepsilon_e})} < v_0 < \frac{r_e\varepsilon_e v_e}{\beta+r_e\varepsilon_e}. \tag{43}$$

In Appendix D, we show that it is always possible to find an initial voltage that obeys this inequality.

Equation (41) is solved by

$$A = \mathrm{LW}(-be^{-b}) + b, \tag{44}$$

where $\mathrm{LW}(x)$ denotes the Lambert W function [24] and b has to be larger than one, as stated above [26]. Replacing A in the latter equation by $\varepsilon_e(1-e^{-t_m/\tau_e})$ leads to an equation for the position of the extremum as follows:

$$t_m = -\tau_e \ln\left\{1-\frac{1}{\varepsilon_e}[\mathrm{LW}(-be^{-b})+b]\right\}. \tag{45}$$

For $b\approx 1$ (leading to $t_m \ll \tau_e$ by making the absolute value of the logarithm small), this equation can be approximated by

$$t_m \approx -\tau_e \ln\left[1-\frac{2}{\varepsilon_e}\left(\frac{1}{r_e\varepsilon_e}\frac{v_0\beta}{v_0-v_e}+1\right)\right]. \tag{46}$$

The same result can be obtained by assuming small times $t_m \ll \tau_e$ in Eq. (41).

The first simple conclusion from Eq. (45) is that we have to have a finite filter time τ_e in order to see an extremum at a finite time—the two times t_m and τ_e are directly proportional to each other. This is also in accordance with the white-noise case considered above where we obtained a purely exponential decay without an extremum (i.e., the "extremum" is in this case at $t_m=0$).

We emphasize that the occurrence of a maximum is both due to the multiplicative character of the noise and due to the filtering, since neither the ECA (additive noise but filtered input), Eq. (8), nor the unfiltered (but still multiplicative) variant, Eq. (40), allow for a nonmonotonic behavior.

D. Comparison to numerical simulations

In the following, $\langle V(t)\rangle=\langle v(t)\rangle+E_L$ using Eq. (37) is plotted for different parameter sets. Our results are compared with the prediction of the ECA and the asymptotic value found by Richardson and Gerstner [11] as well as with numerical simulations of Eqs. (1) and (2). For this purpose, a simple Euler integration scheme has been used. The Poisson input was generated by drawing a uniformly distributed random number between 0 and 1 in each time step. If the random number was smaller than $r_e\Delta t$ the conductance was increased by the value c_e. Most of the parameters from our standard set given in Table I are adopted from Richardson and Gerstner [11]. Different parameter values are indicated in the figure captions.

Figure 3(a) shows the exact result for the time-dependent mean value together with simulation results and the predictions of the ECA for this parameter set. All the curves agree well for the comparably large initial value; there are small

TABLE I. Standard parameter set.

Parameter	Value
r_e	1000 Hz
τ_e	3 ms
c_e	0.034 mS/cm^2
E_e	−65 mV
E_L	−80 mV
C	1 μF/cm^2
g_L	0.05 mS/cm^2
V_0	−50 mV

differences in the asymptotic value, which cannot be seen in the plot, because of the large voltage scale. The good asymptotic agreement can be expected, because the conductance change caused by a single spike is small [smaller than the leak conductance, in accordance with Eq. (10)]. However, in the transient behavior qualitative deviations can still be found. This is demonstrated in Fig. 3(b), where the initial value is set to approximately the steady-state mean value. Now, the exact curve shows clearly a nonmonotonic time curve.

The mean first increases [it follows the ECA curve for a short period as expected from Eq. (11)], reaches a maximum, and then drops toward an asymptotic value which is *below* the initial value V_0 as well as *below* the asymptotic value as

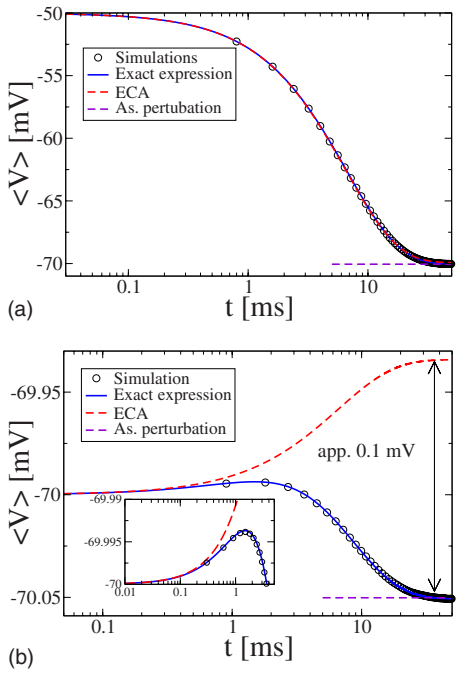

FIG. 3. (Color online) Mean value as a function of time: theory (solid line) according to $\langle V(t)\rangle = E_L + \langle v(t)\rangle$ and Eq. (37); simulations (symbols) performed as explained in the text; steady-state mean (dashed line) according to the perturbation result Eq. (12) by Richardson and Gerstner [11]. Parameters are given in Table I; the initial voltage in (b) is $V_0 = -70$ mV. The simulations are averaged over 10^5 trajectories [panel (a)] and 10^7 trajectories [panel (b)], respectively.

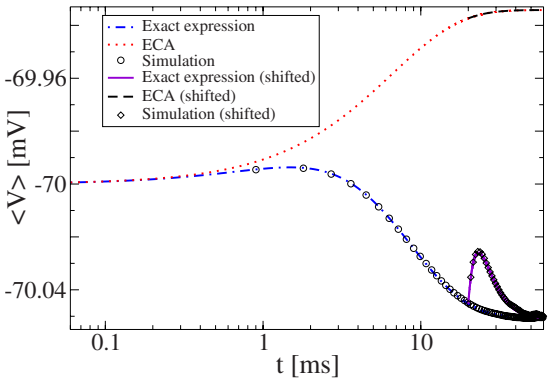

FIG. 4. (Color online) In addition to the curves from Fig. 3(b), the same quantities are plotted for a new initial value $V_0' = \langle V(20\ \text{ms})\rangle$ and time shifted by 20 s, respectively. All other parameters are identical with the ones from Fig. 3(b). The modified solution for the ECA lies exactly on the original one, whereas the exact solutions differ strongly. However, the asymptotic values for the exact solutions are identical.

predicted by the ECA. We emphasize that the ECA predicts always an exponential time course for the mean value and is thus qualitatively wrong for this example. Despite the small quantitative deviation (roughly 0.1 mV), observing such a maximum could be helpful for the estimation of parameters. The prediction of the perturbation expansion of Richardson and Gerstner [11] is in excellent agreement with the exact asymptotic value.

Another striking difference is related to the choice of the initial value. If the initial value for the ECA prediction $\langle V(t)\rangle_{ECA}$ would be reset to a new value somewhere on the curve, $V_0 \rightarrow \langle V(t_1)\rangle_{ECA}$ (note the reset indicated by a change of color in the ECA curve in Fig. 4), one would expect to obtain essentially the same function, solely shifted by $-t_1$. Put differently, starting from a large negative value V^* below the asymptotic mean voltage E_0, the curve passes through all possible curves with initial values between V^* and E_0—there is no new information in choosing another initial value in the linear approximation. However, if this procedure is repeated with the *exact solution* $\langle V(t)\rangle$, this is not the case. The curve with the new initial value deviates from the original curve in the beginning as clearly seen in Fig. 4: the reset curve shows even a more pronounced maximum than the original curve. However, the original function and the one obtained by a reset voltage tend to the same asymptotic value.

From the above considerations, the question arises whether one can find parameter sets where the quantitative deviations are more pronounced. In Sec. I C, the limitations of the ECA have been discussed. This can be used to identify such sets. One example can be constructed by setting r_e to 20 Hz, c_e to 2 mS/cm^2, τ_e to 1 ms, and E_e to 0 mV in the standard set; here both inequalities Eqs. (9) and (10) are not obeyed. These values are still in the physiological range and correspond to a neuron with comparably few synaptic connections but a strong effect of a single incoming spike. In this case, the asymptotic deviations become as large as 14 mV [see Fig. 5(a)]. The deviations of the perturbation expansion of Richardson and Gerstner [11] are smaller, however, they still amount to approximately 4 mV. Remarkably, even

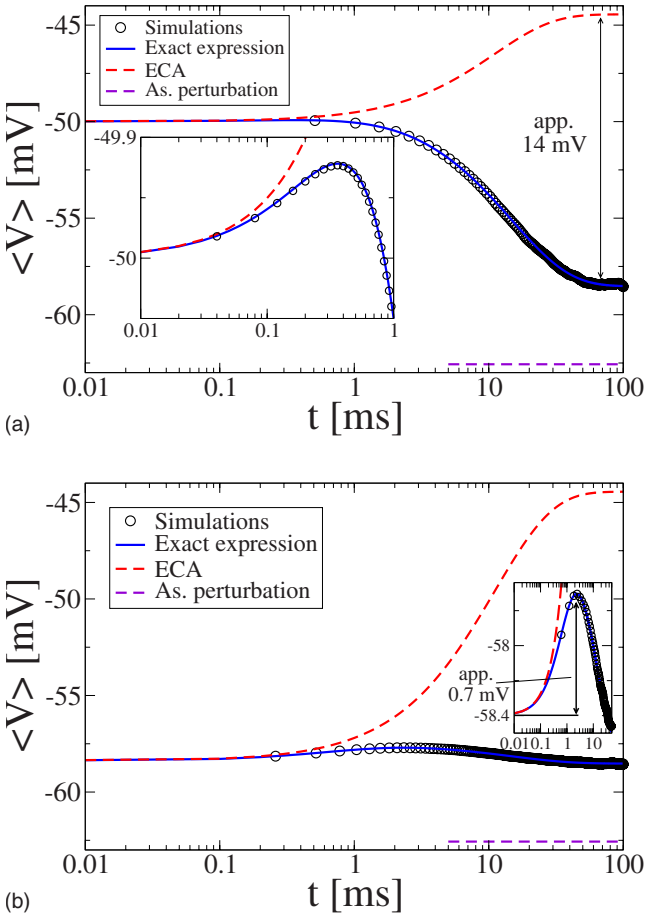

FIG. 5. (Color online) Mean value as a function of time: theory (solid line) according to $\langle V(t)\rangle = E_L + \langle v(t)\rangle$ and Eq. (37); simulations (symbols) performed as explained in the text; steady-state mean (dashed line) according to the perturbation result Eq. (12) by Richardson and Gerstner [11]. Two examples for strong quantitative deviations from the ECA. The changed parameters are $r_e = 20$ Hz, $c_e = 2$ mS/cm^2, $\tau_e = 1$ ms, and $E_e = 0$ mV; the initial voltage in (b) is $V_0 = -58.4$ mV. The simulations are averaged over 10^5 trajectories (main graphs) and over 10^6 trajectories (insets), respectively.

for this particularly large choice of the initial value, a tiny maximum in the time course of the exact mean value can be observed [see the inset in Fig. 5(a)]. Again, by setting the initial value close to the steady-state mean voltage, the maximum gets more pronounced [approximately 0.7 mV in amplitude; see the inset of Fig. 5(b)] and should be observable in experiments.

Another question of interest is, whether the time predicted for the maximum (under the assumption of small times compared to the synaptic time scale), Eq. (46), is in agreement with the exact curves in our examples. This is an important point if one wants to use the position of the maximum as a criterion for the estimation of a parameter (see also the discussions in Sec. IV). In Fig. 3(b), the maximum is at roughly $t = 1.5$ ms and Eq. (46) yields 1.46 ms for these parameters. Here, $\varepsilon_e = 0.102$. For the last example [Fig. 5(a)], $\varepsilon_e = 2$. In this case, the instance of the maximum predicted by Eq. (46) is at $t_m = 0.29$. This is still close to the exact value $t = 0.36$.

The accuracy of Eq. (46) was also checked against the exact solution Eq. (45). In Fig. 6 we show the approximate

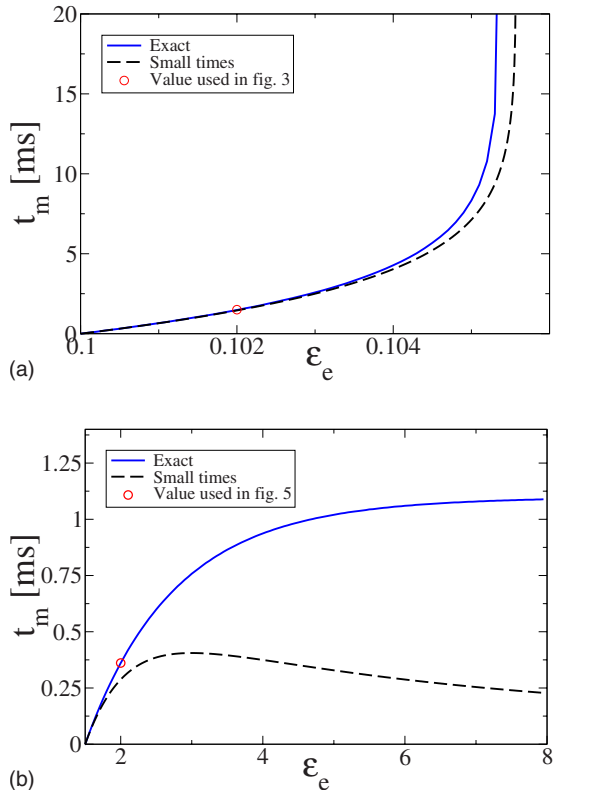

FIG. 6. (Color online) The approximation Eq. (46) (dashed lines) and the exact result Eq. (45) for t_m, plotted vs ε_e. The parameters are taken for panel (a) from Fig. 3(b) and for panel (b) from Fig. 5(a).

and the exact values of t_m as a function of the parameter ε_e for our examples from Figs. 3(b) and 5(a). As can be seen, in both cases a maximum can only occur for sufficiently strong ε_e [$\varepsilon_e > 0.1$ in (a), $\varepsilon_e > 1.5$ in (b)]. The approximation of t_m works well for small ε_e; for larger ε_e the maximum may vanish again [note the divergence for large ε_e in Fig. 6(a)] or saturate [Fig. 6(b)]. For values of ε_e in the physiological range (see, e.g., circles in Fig. 6) our results indicate that Eq. (46) provides a good approximation for the time instant of maximal mean voltage.

IV. CONCLUSIONS AND DISCUSSIONS

We presented a method to calculate arbitrary moments for the subthreshold fluctuations of a shot-noise-driven passive neuron. In a simple example, parameter regions were identified where the effective time-constant approximation (ECA) is not sufficient. In the example, the shot-noise input was considered as Poissonian and only excitatory synapses have been taken into account. The exact mean value for this example was compared to predictions of the ECA and to simulation results. Note that the evaluation of Eq. (37) by a *C* program takes roughly 30 s, whereas the simulations have to run for up to 40 h, depending on the desired accuracy.

We found systematic deviations from the predictions of the ECA in (i) the asymptotic value of the voltage (e.g., whether it is smaller or larger than the initial voltage, cf. Fig.

5), (ii) the time course which can be nonmonotonic, and (iii) the dependence on a reclamping of the voltage (cf. Fig. 4). For a small and purely excitatory drive, we could identify conditions leading to a nonmonotonic mean as a function of time. Preliminary results indicate that also the time-dependent standard deviation can show extrema and that strong quantitative deviations of the ECA can appear. As the ECA replaces the original shot noise by a Gaussian process, it neglects the nontrivial higher moments of the shot noise. Thus, the difference between the exact solution and the ECA should be even larger for higher moments, as was shown by Richardson and Gerstner [11] for the skew of the steady-state voltage distribution.

The extrema which can show up in the time course of the mean value may also be helpful for the estimation of parameters. In the case of the ECA, there are only two effective parameters, namely, the effective reversal potential E_0 and the effective timescale τ_0. With the equation for the position of the maximum, Eq. (46), we have an additional condition for parameter estimation. If now extrema are discovered also in higher moments, they might allow for the determination of even more parameters. As an example, we used Eq. (46) to determine the synaptic time scale from simulations of the full dynamics at our standard parameter set (Table I) with an inital voltage of −70 mV. To have realistic conditions, we used an ensemble of 62 500 trajectories and a simulation time of 8 ms. This leads to a total time for one measurement of less than 9 min. To obtain an estimate for the statistical error, we estimated τ_e ten times from different runs of the simulation. The mean over the ten runs was (3.2 ± 0.4) ms. The error for one measurement is indicated. The true value for τ_e is 3 ms and the relative error therefore amounts to 13%.

In this paper we have assumed a passive membrane, i.e., we have neglected any voltage-dependent conductances and thus a spiking mechanism. Clearly, spiking would distort the voltage statistics, overriding some if not all of the subtle effects we found in this paper. Our results apply only to situations where no or almost no spiking occurs. This is the case, for instance, if the main voltage-dependent channels are chemically blocked or if the neuron is strongly hyperpolarized by an additional current. Last but not least, it also corresponds to a weak input, insufficient to cause firing or to a dominating inhibitory input.

Another neglected feature is the spatial extension of the neuron. We assume that the postsynaptic potential (PSP) does not change qualitatively on its way from the dendrite to the soma. In many neurons, for instance motoneurons in the rat's spinal cord [25], the dendritic membrane is largely passive and the PSP is solely reduced in amplitude and is low-pass filtered. This could be accounted for in our model by a change in the synaptic time scale $\tau_{e,i}$ and the amplitude $c_{e,i}$; an effective bandpass filtering could be included by a higher-order synaptic filter.

Our method calls for many more applications. An interesting question is whether for excitatory and inhibitory input being present, the time-dependent mean value can show two or more extrema and how parameter values can be extracted in this more complicated case.

Moreover, our method can be also used to calculate the autocorrelation function of the voltage fluctuations. This function can be obtained experimentally from a long voltage trajectory (without repeated reclamping of the voltage) and thus simplifies the comparison to experiments.

Another important point for further extensions of this solution concerns the choice of the filter function. The function $G_{e,i}$ in Eqs. (30) and (31) is the Green's function of the filter dynamics equation (2). This implies that another (more realistic) filter could be included simply by replacing the function $G_{e,i}$ by the Green's function of the new filter dynamics. The other parts of Eqs. (30) and (31) will not be affected. A linear filter which takes into account the finite rise time of the conductance is, for example, the α function, which is proportional to $t \exp[-\alpha t]$. In general, more realistic filters possess more complicated Green's functions. This in turn will lead to more complicated integrals in the final expression, for instance, in those appearing in the time-dependent mean value.

Finally, we emphasize that the formulas derived in Sec. II are valid for both inhibitory and excitatory input, and can be used for all kinds of stationary input point processes, as long as their generating or characteristic functional can be calculated. This permits the use of more realistic (i.e., correlated) shot noise, which is a particularly exciting subject of future research.

APPENDIX A: THE MEAN AT SHORT TIMES

Here we show that the ECA dynamics around the initial value is completely equivalent to the full dynamics [Eqs. (1) and (2)], i.e., we prove Eq. (11). At $t=0$, $V=V_0$ and the statistics of the voltage is independent of the conductances. Thus, the mean of Eq. (1) can easily be taken, yielding

$$\left.\frac{d\langle V\rangle}{dt}\right|_{t=0} = \frac{1}{C}[-(V_0-E_L)g_L-(V_0-E_e)\langle g_e\rangle-(V_0-E_i)\langle g_i\rangle]. \tag{A1}$$

The mean of Eq. (6) for $t=0$ yields (where we omit all terms with zero mean)

$$\begin{aligned}\left.\frac{d\langle V\rangle_{ECA}}{dt}\right|_{t=0} &= \frac{1}{C}[-(V_0-E_0)g_0] \\ &= \frac{1}{C}[-(V_0-E_L)g_L-(V_0-E_e)g_{e0} \\ &\quad -(V_0-E_i)g_{i0}].\end{aligned} \tag{A2}$$

By construction, $g_{e0,i0}=\langle g_{e,i}\rangle$, and thus Eq. (11) results.

APPENDIX B: EVALUATION OF THE EXPRESSIONS FOR THE EXACT MOMENTS

In this Appendix, we show that the crucial step to calculate the moments is to evaluate expression (20). To keep the expressions readable, we do this only for moments up to second order, i.e., the autocorrelation function. The explicit definition reads

$$\begin{aligned}\langle v(t)v(t+\tau)\rangle &= \left\langle \left(v_0 e^{-\beta t} \exp\left\{ -\int_0^t du[y_e(u)+y_i(u)] \right\} + \int_0^t ds[v_e y_e(s)+v_i y_i(s)] e^{-\beta(t-s)} \exp\left\{ -\int_s^t du[y_e(u)+y_i(u)] \right\} \right) \right. \\ &\quad \times \left(v_0 e^{-\beta(t+\tau)} \exp\left\{ -\int_0^{t+\tau} du'[y_e(u')+y_i(u')] \right\} + \int_0^{t+\tau} ds'[v_e y_e(s')+v_i y_i(s')] e^{-\beta(t+\tau-s')} \right. \\ &\quad \left. \left. \times \exp\left\{ -\int_{s'}^{t+\tau} du'[y_e(u')+y_i(u')] \right\} \right) \right\rangle \\ &= \left\langle v_0^2 e^{-\beta(2t+\tau)} \exp\left\{ -\int_0^t du[y_e(u)+y_i(u)] - \int_0^{t+\tau} du[y_e(u)+y_i(u)] \right\} \right\rangle \\ &\quad + \left\langle v_0 \int_0^{t+\tau} ds' e^{-\beta(2t+\tau)}[v_e y_e(s')+v_i y_i(s')] \exp\left\{ -\int_0^t du[y_e(u)+y_i(u)] - \int_{s'}^{t+\tau} du[y_e(u)+y_i(u)] \right\} \right\rangle \\ &\quad + \left\langle v_0 \int_0^t ds e^{-\beta(2t+\tau)}[v_e y_e(s)+v_i y_i(s)] \exp\left\{ -\int_s^t du[y_e(u)+y_i(u)] - \int_0^{t+\tau} du[y_e(u)+y_i(u)] \right\} \right\rangle \\ &\quad + \left\langle \int_0^t ds \int_0^{t+\tau} ds' e^{-\beta(2t+\tau-s-s')}[v_e y_e(s)+v_i y_i(s)][v_e y_e(s')+v_i y_i(s')] \right. \\ &\quad \left. \times \exp\left\{ -\int_s^t du[y_e(u)+y_i(u)] - \int_{s'}^{t+\tau} du'[y_e(u')+y_i(u')] \right\} \right\rangle. \end{aligned} \tag{B1}$$

To do the averaging and obtain expression (20), the exponentials have to be split into a product of terms which only contain either y_e or y_i, and the conductances multiplying the exponential have to be replaced by derivatives. Thus, the averaging has to be done over terms like

$$\frac{d}{ds}\exp\left[-\int_s^{t_1} du y_e(u) - \int_{s'}^{t_2} du y_e(u) \right] \frac{d}{ds'}\exp\left[-\int_s^{t_1} du y_i(u) - \int_{s'}^{t_2} du y_i(u) \right]. \tag{B2}$$

If we now assume the excitatory and inhibitory noise to be uncorrelated, we can write the expectation value of the product as the product of expectation values as follows:

$$\begin{aligned}&\left\langle \frac{d}{ds}\exp\left[-\int_s^{t_1} du y_e(u) - \int_{s'}^{t_2} du y_e(u) \right] \frac{d}{ds'}\exp\left[-\int_s^{t_1} du y_i(u) - \int_{s'}^{t_2} du y_i(u) \right] \right\rangle \\ &\quad = \frac{d}{ds}\left\langle \exp\left[-\int_s^{t_1} du y_e(u) - \int_{s'}^{t_2} du y_e(u) \right] \right\rangle \frac{d}{ds'}\left\langle \exp\left[-\int_s^{t_1} du y_i(u) - \int_{s'}^{t_2} du y_i(u) \right] \right\rangle. \end{aligned} \tag{B3}$$

Clearly, this expression is of the form given in Eq. (20).

APPENDIX C: EVALUATION OF f_e

With some simple shifts of the integration variables, namely, $t' \to t'' = t' - s$ and $u \to u' = u - s$, one can see that f_e only depends on the difference of the arguments as follows:

$$\begin{aligned} f_e(t,s) &= r_e \int_{-\infty}^{+\infty} du (e^{-\int_s^t dt' G_e(t'-u)} - 1) \\ &= r_e \int_{-\infty}^{+\infty} du' (e^{-\int_0^{t-s} dt'' G_e(t''-u')} - 1) = f_e(t-s). \end{aligned} \tag{C1}$$

The index e will be suppressed throughout the following. According to Eq. (35), we have to calculate

$$f(t) = r\int_{-\infty}^{\infty} du(e^{-\int_0^t dt' G(t'-u)} - 1), \tag{C2}$$

with $G(t'-u)$ given by Eq. (23). To do the outer integration, we have to know the value of the exponential's argument, in the following called $\mathcal{I}$, for all u:

$$\mathcal{I} = -\int_0^t dt' H(t'-u)\frac{\varepsilon}{\tau}e^{-(t'-u)/\tau}. \tag{C3}$$

Because of the Heaviside function $H(x)$ it is convenient to split the integration over u into three integrals over $u<0$, $0\le u\le t$, and $u>t$. For $\mathcal{I}$ we obtain

$$\mathcal{I} = \begin{cases} \varepsilon e^{u/\tau}(e^{-t/\tau}-1) & u<0 \\ \varepsilon(e^{-(t-u)/\tau}-1) & 0\le u\le t \\ 0 & u>t. \end{cases} \tag{C4}$$

We can now write for f,

$$f(t) = r\left(\underbrace{\int_{-\infty}^{0} du(e^{\varepsilon e^{u/\tau}(e^{-t/\tau}-1)} - 1)}_{=I_1} + \underbrace{\int_0^t du(e^{\varepsilon(e^{-(t-u)/\tau}-1)} - 1)}_{=I_2} + \underbrace{\int_t^{\infty} du(e^0 - 1)}_{=0}\right). \tag{C5}$$

The remaining task is to calculate the two integrals. For this purpose, we use the following relation:

$$\int^x dx' \exp[\beta e^{\alpha x'}] = \frac{1}{\alpha}\mathcal{E}i[\beta e^{\alpha x}]. \tag{C6}$$

I_2 yields

$$I_2 = \tau(\mathcal{E}i[\varepsilon] - \mathcal{E}i[\varepsilon e^{-t/\tau}])e^{-\varepsilon} - t. \tag{C7}$$

For I_1, there is a difficulty, caused by the logarithmic divergence of $\mathcal{E}i[x]$ at $x=0$. Therefore, we write it as the limit of a proper integral as follows:

$$I_1 = \lim_{C\to\infty}\int_{-C}^{0} du(e^{\varepsilon e^{u/\tau}(e^{-t/\tau}-1)} - 1) \overset{\text{Eq. (C6)}}{=} \lim_{C\to\infty}\{\tau\mathcal{E}i[\varepsilon(e^{-t/\tau}-1)e^{u/\tau}] - u\}_{-C}^{0} = \tau\lim_{C\to\infty}\left(\mathcal{E}i[\varepsilon(e^{-t/\tau}-1)] - \mathcal{E}i[\varepsilon(e^{-t/\tau}-1)e^{C/\tau}] - \frac{C}{\tau}\right). \tag{C8}$$

For very large C, the factor $e^{-C/\tau}$ and thus the argument of the $\mathcal{E}i[\,]$ function gets very small. This function can be expanded around zero as follows:

$$\mathcal{E}i[x] \overset{x\ll 1}{\approx} \ln[|x|] + \gamma, \tag{C9}$$

with γ being the Euler-Mascheroni constant, $\gamma = 0.577\,215\,66\ldots$.

Thus,

$$\begin{aligned} I_1 &= \tau\left\{\mathcal{E}i[\varepsilon(e^{-t/\tau}-1)] - \lim_{C\to\infty}\left(\ln[\varepsilon(1-e^{-t/\tau})e^{-C/\tau}] + \gamma + \frac{C}{\tau}\right)\right\} \\ &= \tau\left\{\mathcal{E}i[\varepsilon(e^{-t/\tau}-1)] - \lim_{C\to\infty}\left(\ln[\varepsilon(1-e^{-t/\tau})] + \gamma - \frac{C}{\tau} + \frac{C}{\tau}\right)\right\} \\ &= \tau\{\mathcal{E}i[\varepsilon(e^{-t/\tau}-1)] - \ln[\varepsilon(1-e^{-t/\tau})] - \gamma\}. \end{aligned} \tag{C10}$$

Altogether, f reads

$$\begin{aligned} f(t) = r\tau\{&\mathcal{E}i[\varepsilon(e^{-t/\tau}-1)] + (\mathcal{E}i[\varepsilon] - \mathcal{E}i[\varepsilon e^{-t/\tau}])e^{-\varepsilon} \\ &- \ln[\varepsilon(e^{t/\tau}-1)] - \gamma\}. \end{aligned} \tag{C11}$$

APPENDIX D: CONDITIONS FOR THE NONMONOTONIC MEAN

By examining the conditions, one can see that one can always find an initial value which fulfills the inequalities (43): By using the fact that both the right-hand side and the left-hand side of the inequality (43) share the structure

$$F(A) = \frac{r_e v_e A(\varepsilon_e)}{\beta + r_e A(\varepsilon_e)}, \tag{D1}$$

which is increasing strictly monotonically with A, and using that

$$(1-e^{-\varepsilon_e}) < \varepsilon_e \quad \forall \quad \varepsilon_e > 0, \tag{D2}$$

one can easily show that the left-hand side of the inequality (43) is always smaller than the right-hand side. This proves that it is always possible to find an initial value which leads to a nonmonotonic time course of the mean.

[1] G. Silberberg, C. Wu, and H. Markram, J. Physiol. (London) **556**, 19 (2004).
[2] A. Destexhe, M. Neubig, D. Ulrich, and J. Huguenard, J. Neurosci. **18**, 3574 (1998).
[3] A. V. Holden, *Models of the Stochastic Activity of Neurones* (Springer Verlag, Berlin, 1976).
[4] R. B. Stein, Biophys. J. **7**, 37 (1967).
[5] P. Johannesma, in *Neural Networks*, edited by E. Caianiello (Springer, Berlin, 1967), p. 116.
[6] P. Lánský and V. Lánská, Biol. Cybern. **56**, 19 (1987).
[7] H. C. Tuckwell, *Stochastic Processes in the Neurosciences* (SIAM, Philadelphia, 1989).
[8] B. Lindner and A. Longtin, Neural Comput. **18**, 1896 (2006).
[9] A. N. Burkitt, Biol. Cybern. **85**, 247 (2001).
[10] A. N. Burkitt, Biol. Cybern. **95**, 1 (2006).
[11] M. Richardson and W. Gerstner, Neural Comput. **17**, 923 (2005).
[12] M. R. Deweese and A. M. Zador, J. Neurophysiol. **92**, 1840 (2004).
[13] M. Rudolph, Z. Piwkowska, M. Badoual, T. Bal, and A. Destexhe, J. Neurophysiol. **91**, 2884 (2004).
[14] N. Brunel and S. Sergi, J. Theor. Biol. **195**, 87 (1998).
[15] H. C. Tuckwell, J. Theor. Biol. **77**, 65 (1979).
[16] P. Dayan and L. F. Abbott, *Theoretical Neuroscience* (MIT Press, Cambridge, MA, 2001).
[17] A. Destexhe, Z. F. Mainen, and T. J. Sejnowski, J. Comput. Neurosci. **1**, 195 (1994).
[18] A. N. Burkitt and G. M. Clark, Neural Comput. **11**, 871 (1999).
[19] E. Muller, L. Buesing, J. Schemmel, and K. Meier, Neural Comput. **19**, 2958 (2007).
[20] M. J. E. Richardson, Phys. Rev. E **69**, 051918 (2004).
[21] R. L. Stratonovich, *Topics in the Theory of Random Noise* (Gordon and Breach, New York, 1967).
[22] M. O. Caceres and A. A. Budini, J. Phys. A **30**, 8427 (1997).
[23] C. W. Gardiner, *Handbook of Stochastic Methods* (Springer-Verlag, Berlin, 2004).
[24] R. Corless, G. Gonnet, D. Hare, D. Jeffrey, and D. Knuth, Adv. Comput. Math. **5**, 329 (1996).
[25] M. E. Larkum, T. Launey, A. Dityatev, and H.-R. Lüscher, J. Neurophysiol. **80**, 935 (1998).
[26] The principal branch of the Lambert W function is the inverse function of $y=xe^x$ for $x\geq -1$. If one extends the range of definition for the latter function to arguments smaller than minus one, the function is not monotonic anymore. Thus, one can divide the range of definition in two sets ($x\leq -1$ and $x\geq -1$), where different inverse functions are valid. Both inverse functions agree for $x=-1$. In our case, $x=-b\leq -1$ and thus the principal branch of the Lambert W function is *not* the inverse function. Therefore, the trivial identity $A=-b+b=0$ is only fulfilled in the limit $b\rightarrow -1$.